MASKLESS FABRICATION OF HIGH ASPECT RATIO STRUCTURES BY COMBINATION OF MICROMOLDING AND DIRECT DRAWING

Jooncheol Kim, Seung-Joon Paik, Po-Chun Wang, Seong-Hyok Kim, and Mark G. Allen
School of Electrical and Computer Engineering, Georgia Institute of Technology, Atlanta, Georgia, USA

ABSTRACT

This paper presents a fabrication process combining micromolding and direct drawing, and its application to the development of high aspect ratio microneedles. Without using photolithography or etching, the proposed process creates microneedles with: 1) higher aspect ratios than that of the original mold, 2) controllable needle diameter for optimized mechanical strength, and 3) arrowhead-shaped tips for potentially increased capacity and effective payload delivery. The needles presented are formed with biocompatible, water-soluble polymers, but the fabrication process inherently allows many kinds of polymers to be exploited. Various high aspect ratio 3D structures were fabricated and characterized, and the fabrication result was compared with theoretical prediction. Water-soluble microneedle arrays have been fabricated and successfully penetrated into porcine skin, fully releasing the drug-surrogate into the dermis layer within a minute.

INTRODUCTION

Three-dimensional pattern transfer and direct drawing lithography are attractive processes due to their simplicity as well as their ability to achieve high aspect ratio structures [1, 2]. Micromolding processes use non-covalent surface forces to transfer patterns from high aspect ratio polydimethylsiloxane (PDMS) mold to polymeric replicates [1]. While many micromolding processes have demonstrated successful three-dimensional pattern transfer, most are limited to direct replication of the mold master as shown in Figure 1(a). Drawing lithography produces high aspect ratio structures directly from a flat surface [2] by exploiting the necking phenomenon [3], yielding structures of non-complex, yet highly repeatable geometries as shown in Figure 1(b). If the polymer is drawn from a micromold instead of a flat surface, the produced structures have a higher aspect ratio than the original mold, even with a simple drawing trajectory. Moreover, by controlling the sequence of drawing speeds, length and directions, as well as exploiting the original mold shape, more complex structures can be achieved as described in Figure 1(c).

In this paper, a high aspect ratio structure fabrication process using a combination of micromolding and direct drawing is outlined. This process combines the high aspect ratios achievable from direct drawing with the designed shapes of microfabricated molds. The fabrication process utilizes PDMS as a mold material, and a biocompatible, water-soluble polymer for the micro-structure material. As an application of the proposed fabrication process, microneedle arrays are proposed and fabricated. Also, a fracture test and an insertion test into porcine skin have performed to evaluate mechanical strength and skin penetration performance of the fabricated microneedle arrays, respectively.

FABRICATION AND ANALYSIS

Materials Preparation

Several FDA-approved biodegradable polymers such as poly-glycolic acid (PGA), poly-lactic-*co*-glycolic acid (PLGA), carboxymethyl cellulose (CMC), polyvinyl alcohol (PVA), and polyvinyl-pyrrolidone (PVP) are suitable candidates for dissolving microneedles due to their sufficient mechanical strength for insertion and drug encapsulation-release controllability [4-6]. In this experiment, an aqueous mixture of PVA, PVP and water with a weight ratio of 1:1:2 was used for the microstructure material. The polymer is dyed with a sulforhodamine B solution as a drug-surrogate. Various materials commonly used in MEMS fabrication that have appropriate viscosity and are capable of being solidified can be applicable for this process.

Fabrication Process

Inclined rotational photolithography is used for the fabrication of a reusable PDMS mold which contains 10×10 arrays of Ø400μm×500μm conical trenches [7]. The water-soluble polymer is cast onto the PDMS mold and the cast polymer is subjected to a vacuum through the PDMS mold for 30 minutes to remove entrapped air bubbles. The mold is then spun at 3000 rpm for 15 seconds to achieve a flat surface of the polymer. As the cast polymer dries, it is observed that the top surface of the polymer solidifies

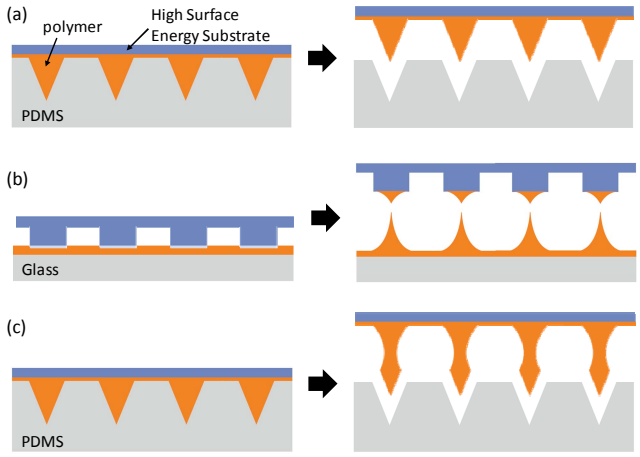

Figure 1: (a) Conventional replica 3D micro molding process. (b) Conventional drawing lithography for 3D high aspect ratio structure. (c) Proposed fabrication process which combines micromolding and direct drawing for shape-controllable 3D high aspect ratio structure.

before the polymeric material deep in the molds. This effect is exploited by drying the surface of the cast polymer in a hood for approximately 25 minutes prior to attachment of a high surface energy substrate, TM9942 (MACtac, Canada), to this solidified surface. Finally, the drawing process is performed with drawing parameters controlled to achieve the desired various shapes of 3D structures.

Design of Drawing Strategy

A drawing apparatus was designed to control the pulling speed, time, and direction. By adjusting these parameters, various shapes of 3D structures are achievable. Three manipulation scenarios for the proposed fabrication process are described in Figure 2. Simple direct drawing leads to aspect ratio amplification of the original polymer shape, which was originally confined in the mold due to its viscosity as described in Figure 2(a). In this case, drawing is finished when the polymer is naturally separated from the PDMS mold, which enables the very high aspect ratio 3D structure. Including one or more hold steps or push-pull steps in the drawing processes produces the arrowhead-tipped microneedles shown in Figures 2(b) and (c). By holding the drawing process at a certain process step for the polymer to solidify for a certain time, an arrow shaped microneedle, which could be beneficial for delivery of large quantities of drug, is achieved as shown in Figure 2(b). Holding should be maintained until the polymer is fully dried to prevent unwanted elongation of the polymer in the mold. Figure 2(c) describes arrow tip microneedles with reinforced mechanical strength. The microneedles are fabricated by advanced drawing with stop-hold and push-pull steps. In this case, an additional push-down process, rather than holding, is executed immediately after stopping at a desired position. Then, subsequent pulling-up and stop-hold processes are performed which yield a thicker and stronger base with larger tip volume than the conventional drawing process described in Figures 2(a) and (b).

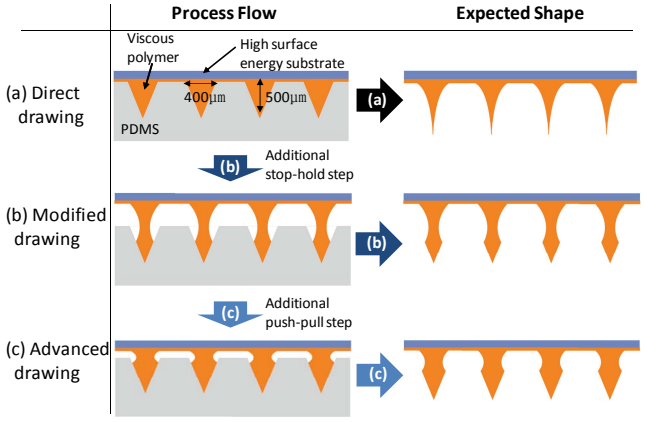

Figure 2: Various fabrication scenarios. (a) Direct drawing for aspect ratio amplification. (b) Modified drawing with stop-hold step to allow shaped microneedle. (c) Advanced drawing with stop-hold and push-pull steps for mechanical strength intensified microneedle.

Fabrication Results

Fabricated 3-D structure arrays realized using the suggested processes are shown in Figure 3. Figure 3(a) describes a direct-drawn 1200μm-tall, sharp-tipped structure. The resulting aspect ratio of 1:3 shows 2.4× amplification from the mold's aspect ratio of 1:1.25. A modified drawing process, incorporating a stop-and-hold sequence, provides an arrowhead-shaped microneedle with a tip volume of 7.5nl, 960μm height, and a minimum necking diameter of 106μm (Figure 3(b)). The process is further enhanced by adding stop-and-hold and push-pull drawing steps to improve the mechanical properties of the structure (Figure 3(c)). The improved arrowhead-shaped microneedle has 9.7nl tip volume, 800μm height, and a minimum necking diameter of 240μm.

Theoretical Analysis

The polymer experiences a necking phenomenon during the drawing process, which results in a rapid decrease of the cross-sectional area at a particular axial position. In the case of a cylindrical shape, the decreasing radius at the narrowest part of the necking zone is strongly time-dependent [3]. As indicated in Figure 4, if a moving coordinate system fixed at the center of the necking zone is chosen, the profile of the radius can be described as a function of time. With the assumption that the polymer volume is constant during the drawing, the minimum radius

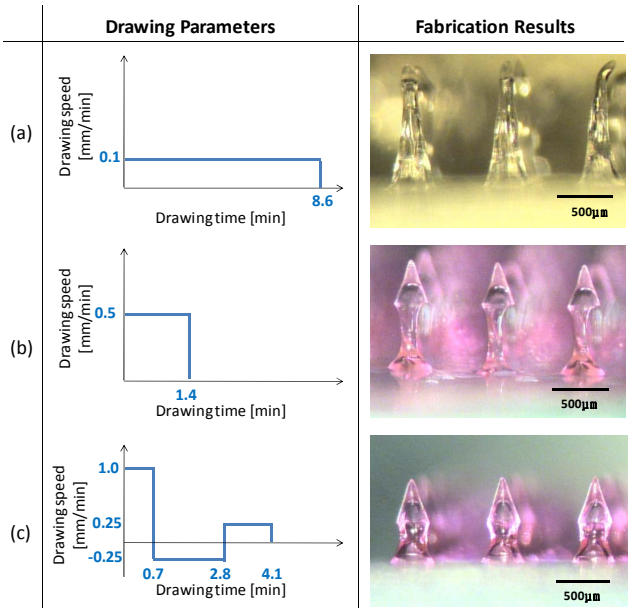

Figure 3: Fabricated 3D structure arrays with various process parameters. (a) 2.4× amplified aspect ratio microneedle by direct drawing (constant drawing at 0.1mm/min for 8.6min). (b) Arrowhead-shaped microneedle by modified drawing (constant drawing at 0.5mm/min for 1.4min). (c) Larger head volume and thicker wall microneedle by advanced drawing (various drawings at 1.0mm/min, -0.25mm/min, and 0.25mm/min for 0.7min, 2.1min, and 1.4min, respectively).

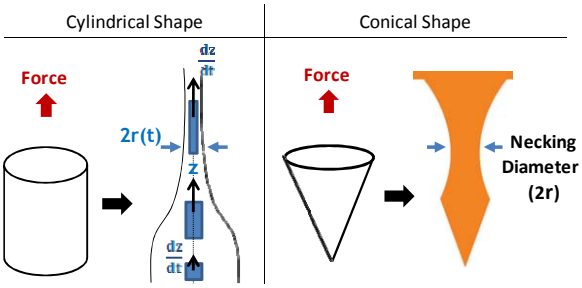

Figure 4: Deformation of a volume element, in cylindrical and conical shapes, by necking with the profile r(t), and the velocity of dz/dt , respectively.

in the flow zone becomes:

$$r(t) = r(0) \cdot \exp\left(-\frac{\epsilon_H}{2} \cdot t\right) \quad (1)$$

where ϵ_H is the strain rate in the unit of second^{-1}, t is the drawing time in second, and r(0) is the initial radius in the unit of μm. Likewise, if drawing force is applied to a conical structure, the height will be elongated and the radius in the elongated area is expected to decrease due to the necking phenomenon.

Comparison of Fabrication Result to Theoretical Analysis

To compare the fabricated needle radius to the theoretical analysis, three different drawing time processes were performed. The minimum radius decreases with increasing drawing time as indicated in Figure 5(a). The graph in Figure 5(b) demonstrates the best-trend line of the necking-induced minimum radius changes in microneedle geometry when the drawing process is applied. Although the strain rate of 0.028sec^{-1} is slightly different from the strain ratio of 0.017sec^{-1} in the theoretical cylinder model, given the geometrical difference, the trend line is reasonably explained by necking theory.

MICRONEEDLE EVALUATION

Mechanical Strength

Since the buckling force is greatly dependent on the radius and equivalent length, improved microneedles by advanced drawing are expected to show larger buckling force than microneedles fabricated by modified drawing. Figure 6 shows the experimental buckling force test on two types of needle arrays, and the improved microneedle provides a 3.0× increase in mechanical strength.

Insertion and Dissolution Test

Dissolving microneedles are an attractive drug delivery approach to overcome challenges such as large drug volume delivery, and controlled, safe, and single-use simple administration because they are to deliver a wide range of therapeutics, and leave no sharp waste after use [6]. Nevertheless, these previous dissolvable microneedle prototypes have not been able to benefit from the advanced shapes achievable using this process [6, 8]. These arrow shaped dissolvable microneedles are expected to have an

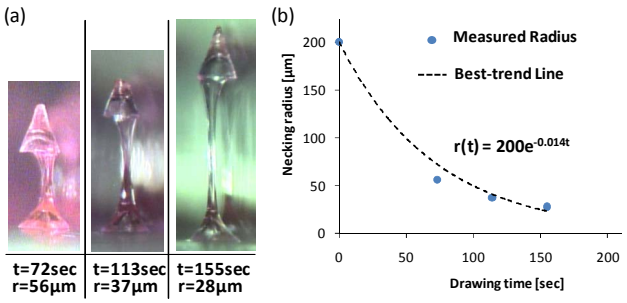

Figure 5: (a) Necking radius decreases with increasing drawing time. (b)The best-trend line of measured conical shape necking data shows that strain rate is derived as 0.028 sec^{-1} which compares reasonably well with the applied value of 0.017 sec^{-1}.

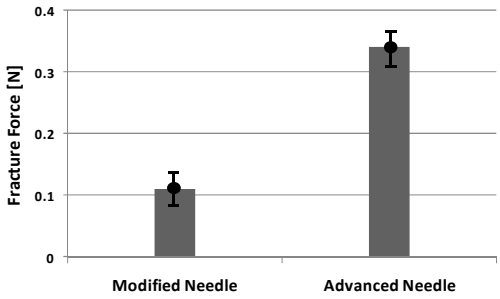

Figure 6: Mechanical fracture test result of microneedle arrays. The advanced drawing provides improved mechanical strength.

advantage of large volume drug delivery over conventional pyramidal or conical dissolvable microneedles. Insertion test of the improved microneedle into porcine skin demonstrated high insertion percentage and successful dissolution of microneedles as shown in Figure 7. For the insertion test, a 10×10 microneedle array (Figure 7(a)) was mounted on the jig assembled into the commercial applicator, Quick-serter (Medtronic Inc., USA), which is currently used for insulin delivery. The applicator can provide uniformly distributed insertion force during the insertion test of microneedle arrays into excised porcine skin. When needles were inserted, they were held for several minutes in order to be dissolved in the skin. After removing the needles, the skin was wiped to remove fluorescent pigment on the surface. Finally, fluorescence was observed only from the penetrated portion of the skin. Figure 7(b) shows that approximately 80 out of 100 fluorescent dyed microneedles penetrated into the skin. Un-inserted portions correspond to the blunt tips observed prior to the insertion test (not shown). The blunt needles were potentially caused by either insufficient vacuum or unexpected particles in the PDMS mold. Figure 7(d) demonstrates that the inserted needles were dissolved within 5 minutes. Even if the array was removed from the skin after 1 minute (Figure 7(c)), the tip part was disconnected so that it still remained and dissolved in the skin. The arrow shape tip assures the anchoring of the microneedle and efficient drug delivery such as in [9].

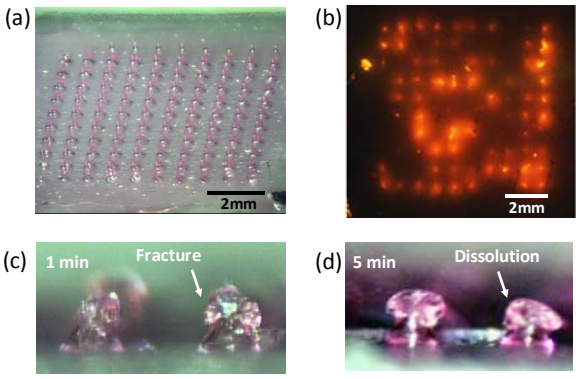

Figure 7: Insertion test into porcine skin (a) Fabricated 10×10 microneedle array. (b) Fluorescent image of the porcine skin after microneedle insertion. (c, d) Magnified views of microneedles after 1min and 5min insertion into the porcine skin, respectively. Needle tip was dissolved in 5 minutes.

Longevity Demonstration

Securing microneedles against unintended use, including reuse, is a key need in clinical application. Water-soluble polymer microneedles possess inherent qualities that achieve the goal. Due to the primarily hygroscopic deterioration of the microneedle when exposed to ambient environment, the microneedle will not function if its packaging has been compromised. Figure 8 shows comparison of the microneedle deformation in a desiccating environment, mimicking appropriate packaging, to that in an uncontrolled ambient environment. In the condition of normal atmosphere, the microneedle is deformed within a day (Figure 8(a)) so that it is no longer applicable for drug delivery. In contrast, Figure 8(b) shows that the microneedles are still intact since they are preserved in absorption desiccating environment.

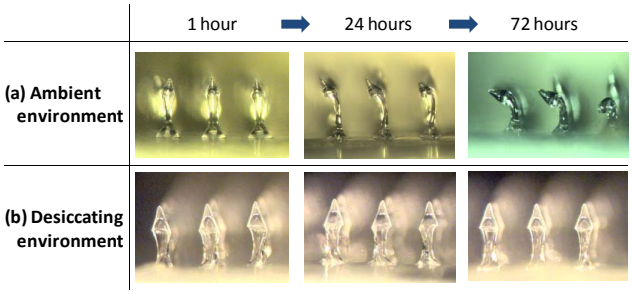

Figure 8: Long-term stability test. (a) When exposed to the uncontrolled ambient environment, the needles are deformed in a day. (b) The needles are still in good shape in the controlled environment.

CONCLUSION

The fabrication process combining micromolding and direct drawing allows 3D high aspect ratio structures to be achieved without lithography or etching. By changing process parameters, high aspect ratio 3D structures with various geometries have been demonstrated, encompassing very high aspect ratio microneedles, arrow-tipped microneedles, and microneedles with controllable mechanical strength and drug-surrogate loading amount. Dissolvable arrow-shaped microneedle arrays show promise for controlled, safe, and high-volume transdermal drug delivery.

ACKNOWLEDGEMENTS

We thank Dr. M.R. Prausnitz, Dr. J.W Lee, and Dr. S.-O Choi at Georgia Institute of Technology for supporting microneedle evaluation. This work was supported by National Institutes of Health under contracts R01-EB006369 and 1U01AI074579.

REFERENCES

[1] Y. Zhao, Y. Yoon, S.-O. Choi, X. Wu, Z. Liu, and M.G. Allen, "Three dimensional metal pattern transfer for replica molded microstructures," *Appl. Phys. Lett*., vol. 94, no. 2, 023301, 2009.

[2] K. Lee, H.C. Lee, D.-S. Lee, and H. Jung, "Drawing lithography: Three-dimensional fabrication of an ultrahigh-aspect-ratio microneedle," *Adv. Mater*., vol. 22, no. 4, pp. 483-486, 2010.

[3] G.R. Strobl, *The Physics of Polymers: Concepts for Understanding their Structures and Behavior*, Springer, pp. 349-385, 1996.

[4] J.-H. Park, M.G. Allen, and M.R. Prausnitz, "Polymer Microneedles for Controlled-Release Drug Delivery," *Pharm. Res.*, vol. 23, No. 5, pp. 1008-1019, 2006.

[5] S.-J. Paik, S.-H. Kim, P.-C. Wang, B. A. Wester, and M.G. Allen, "Dissolvable-tipped, drug-reservoir integrated microneedle array for transdermal drug delivery," in *Tech. Digest MEMS 2010*, Hong Kong, Jan.24-28, 2010, pp. 312-315.

[6] J.W. Lee, J.-H. Park, and M.R. Prausnitz, "Dissolving microneedles for transdermal drug delivery," *Biomaterials*, vol. 29, no. 13, pp 2113-2124, 2008.

[7] Y.-K. Yoon, J.-H. Park, and M.G. Allen, "Multidirectional UV Lithography for Complex 3-D MEMS Structures," *J. Microelectromech. Syst.*, vol. 15, no. 5, pp. 1121-1130, 2006.

[8] L.Y. Chu, S.-O. Choi and M.R. Prausnitz, "Fabrication of dissolving polymer microneedles for controlled drug encapsulation and delivery: Bubble and pedestal microneedle designs," *J. Pharm. Sci*., vol. 99, no. 10, pp. 4228, 2010.

[9] L.Y. Chu and M.R. Prausnitz, "Separable arrowhead microneedle," *J. Control. Release*, 2010, In Press.